

Electrochemical degradation of butyltrimethylammonium bis(trifluoromethylsulfonyl)imide for lithium battery applications

Cite this: *New J. Chem.*, 2014, **38**, 3879

Christopher L. Klug,^{ab} Nicholas J. Bridges,^{*a} Ann E. Visser,^a Stephen L. Crump^a and Eliel Villa-Aleman^a

Ionic liquids (ILs) are being considered as electrolytes for lithium ion batteries due to their low volatility, high thermal stability, and wide electrochemical windows which are stable at the strongly reducing potentials present in Li/Li⁺ batteries. Lithium metal deposition occurs under strongly reducing conditions and the effect that Li metal and any overpotential has on the stability of ILs is important in furthering the application of ILs in lithium based batteries. Here, *N*-butyl-*N*-trimethylammonium bis(trifluoromethylsulfonyl)imide was exposed to various potential differences in order to collect and characterize the volatile products. The IL produced more volatile products when exposed to strong reducing potentials which included reactive products such as hydrogen, alkanes, and amines. Water is a known contributor to hydrogen production in reducing environments, but the IL is also a source of hydrogen. If Li⁺ was present, the preferred pathway of reduction was plating of the lithium onto the working electrode, thus decreasing the reaction rate of degraded ILs.

Received (in Montpellier, France)
10th March 2014,
Accepted 27th May 2014

DOI: 10.1039/c4nj00355a

www.rsc.org/njc

Introduction

In electrochemical applications, the stability of the electrochemical medium and the width of the electrochemical window determine the utility and application. For example, in lithium ion batteries, the electrolyte must remain inert to electrochemical potentials sufficient to reduce lithium ions to metal. Alkyl carbonates were some of the first solvents to be used in lithium ion batteries since they have high dielectric constants and low viscosities.¹ Other electrolyte systems examined for this application include polymer and gel electrolytes.² A particular emphasis in the development of advanced electrolytes for lithium ion batteries is reducing the volatility and flammability associated with alkyl carbonates.

ILs are attractive media for lithium ion batteries since they offer high conductivity, high thermal stability, and wide electrochemical windows. Recent reports show a variety of ways in which ILs have been used in energy storage applications.^{3–6} To overcome the relatively high viscosity of ILs, ILs can be diluted with traditional solvents with little impact on the conductivity.^{7,8}

The electrochemical redox reactions of ILs have also been experimentally investigated to determine the IL decomposition

products. With ILs, it is assumed that the observed electrochemical cathodic and anodic potential limits are associated with the reduction of cations and oxidation of anions, respectively.^{9,10} However, some results show the IL anion bis(trifluoromethylsulfonyl)imide (Tf₂N[−]) undergoes reductive decomposition before the IL cation.¹¹ Based on quantum mechanical calculations for cathodic decomposition products of 1,1-butylmethylpyrrolidinium ([C_{4,1}pyrr][Tf₂N]), Kroon *et al.* propose a range of decomposition products; methylpyrrolidine and a butyl radical, dibutylmethylamine radical *via* ring opening, and butylpyrrolidine and a methyl radical.¹² After [C_{4,1}pyrr][Tf₂N] electrochemical degradation experiments, 1-methylpyrrolidone, octanes, octenes, isobutanol, dibutylmethylamine, and 1-butylpyrrolidine were identified.¹² The reduction reactions for quaternary ammonium-based ILs have been investigated computationally and there are two possible one-electron reduction reactions, one of which includes loss of a propyl group.¹³ The gas phase calculations show that the C–N bond breakage (loss of a propyl group) is energetically favorable over the reduction reaction where the IL cation remains intact.

Previous literature using ILs do not always use term “Ionic Liquid”, but should not be ignored.¹⁴ In this study the use of tetraethylammonium tetrakisfluoroborate ([N_{2,2,2,2}][BF₄]) was used as an electrolyte solvent in acetonitrile diluent, commercially available under the trade name Digirena E. Digirena E is a traditional organic solvent with the addition of an IL as the electrolyte, thus the bulk of the properties are of the acetonitrile solvent. The experiments focused on real life conditions of

^a Savannah River National Laboratory, Aiken, SC 29808, USA.
E-mail: Nicholas.Bridges@SRNL.doe.gov; Tel: +1 803-725-7279

^b Georgia Regents University, Department of Chemistry and Physics, 1120 15th St., Augusta, 30912, USA

temperature between 70–100 °C, and long exposures to very high potential (2.5–30 h of exposure to electrochemical potentials as high as 6 V, no reference point provided). Extensive analysis of the by-products produced includes several multi-step reactions with actively formed intermediates.

The *N*-butyl-*N*-trimethylammonium bis(trifluoromethylsulfonyl)-imide ($[N_{4,1,1,1}][Tf_2N]$) IL has been a particularly promising IL for battery applications,^{15,16} thus our investigation on the effects of charge and current density on the degradation of $[N_{4,1,1,1}][Tf_2N]$ with the addition of a co-solvent, acetonitrile. Headspace gas samples were collected over each half-cell independently. The non-condensable gases were measured by mass spectrometry (MS), and product identities were confirmed with gas chromatography-mass spectrometry (GC-MS) and Fourier transform-infrared spectroscopy (FT-IR). The presence of lithium ion in the system did not affect the reduction reaction, just the rate of production due to the electrochemical deposition of the lithium metal.

Results and discussion

Direct injection mass spectrometry (DI-MS)

An earlier report had shown electrochemical windows for a variety of ILs and a lower cathodic limit of -2.6 V for $[N_{4,1,1,1}][Tf_2N]$ in comparison to -2.4 V for $[C_{4,1}pyrr][Tf_2N]$, vs. ferrocene couple.¹⁷ Other researchers have reported on the stability of quaternary ammonium cations, especially in the presence of lithium salts, such that the cathodic limit allows for battery research to be pursued using $[N_{4,1,1,1}][Tf_2N]$.^{13,16,18} At the potentials used for plating and stripping Li, currents observed in the experimental setup can approach or slightly exceed ± 5 mA. Since many batteries can take a few hours to fully recharge, any materials used in the battery should be able to tolerate currents of several milliamps for several hours.

To examine the effect of variable charge on the degradation of $[N_{4,1,1,1}][Tf_2N]$, ± 5 mA was run for 1, 2, 4, 6, or 8 hours through $[N_{4,1,1,1}][Tf_2N]$ samples diluted with acetonitrile. While there are a number of peaks present in all of the spectra at an m/z less than 45 amu, hydrogen was the only one of these peaks which is due to the degradation of the IL, the other peaks were inert environmental background. Results from the reduction of IL for 8 hours are shown in Fig. 1. Products clearly related to the total charge passed through the system are found at m/z of 2.01, 55.1, 56.1, 57.1, 58.1, 59.1, 69.1, 70.1, 71.2, 72.2, and 101.4 amu.

Other studies using radiolysis indicate that the formation of alkyl moieties from quaternary ammonium cations with and without amine groups is possible.¹⁹ Computationally, the electrochemical reduction of quaternary ammonium cations to an amine and an alkyl radical has also been found to be the most likely reaction. The alkyl radicals could be quenched by the abstraction of hydrogen from neighboring cations. The alkyl and amine products from $[N_{4,1,1,1}][Tf_2N]$ would be volatile and ranging from m/z 16 to as high as 185 amu. The products at m/z 55.1–59.1, 71.2, 72.2, and 101.4 amu are consistent with alkyl, alkenyl, and amine products as described in literature.¹⁹ The fragmentation pattern observed in the mass spectra resembles

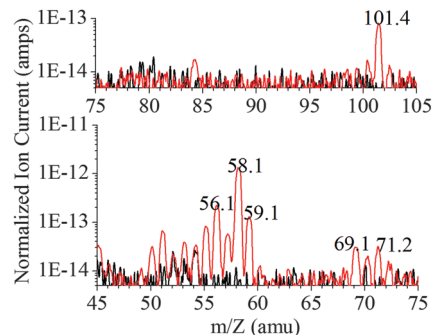


Fig. 1 Effect of variable charge on the reductive degradation of $[N_{4,1,1,1}][Tf_2N]$ with -5 mA for 8 hours (red), compared to the blank (black). All data was normalized to the pressure of each sample.

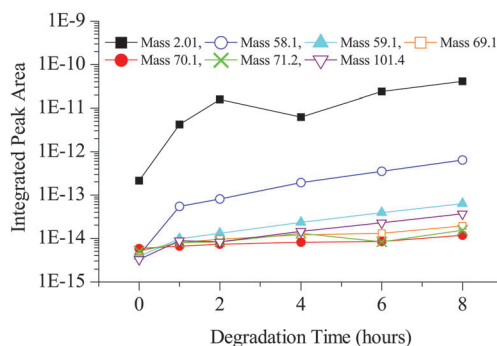


Fig. 2 Effect of charge (-5 mA, variable time) on the concentration of degradation products.

database spectra for fragmentation of butene or butadiene isomers. Mass 71.2 could result from the degradation of the quaternary ammonium cation to form a buteneamine, or it could be from fragmentation of butan-1-amine.²⁰ Increasing the degradation time (total charge) resulted in an exponential increase in the concentration of degradation products as shown in Fig. 2. (The DI-MS was not calibrated for quantification of all the gaseous species measured. The rate of increase of the response from the DI-MS is not guaranteed to be linear to the increase in the quantity of the species.)

Cleavage of the terminal trifluoromethyl group from $[Tf_2N]^-$ would lead to the formation of the CF_3^\bullet radical, which could abstract hydrogen producing a volatile compound. Within the MS, trifluoromethane was observed as CF_3^+ and CF_2H^+ at m/z 69.1 and 51.1 amu, respectively.^{9,20} The formation of trifluoromethane is the only evidence of the anion's degradation and no evidence was observed for the formation of sulfur containing gases or gases that contained nitrogen originating from electrochemical degradation of the $[Tf_2N]^-$ in this study.

The $[N_{4,1,1,1}][Tf_2N]$ diluted with an equal volume of acetonitrile was reduced by constant charge (72 C) over variable times to study the effect of current density on degradation. The normalized integrated peak areas for hydrogen, butane, butene, and trifluoromethane are shown in Fig. 3, illustrating the constant production of degradation gases given constant charge across six different current densities. Within the tested

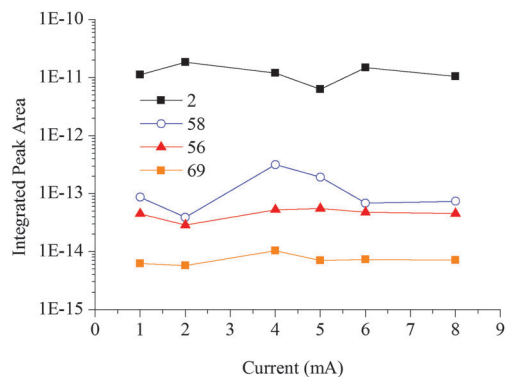


Fig. 3 Effect of current on hydrogen (2), butane (58), butene (56) and trifluoromethane (69) production from reduction of $[\text{N}_{4,1,1,1}][\text{Tf}_2\text{N}]$. All data was normalized to the pressure of each sample, and the maximum measured concentration. Since the product of current and time was set to a constant 20 mA h, and the same foil area was used in each experiment, the current applied is proportional to the current density.

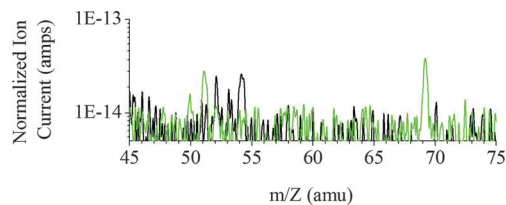


Fig. 4 Effect of variable charge on the oxidative degradation of $[\text{N}_{4,1,1,1}][\text{Tf}_2\text{N}]$ with +5 mA for 8 hours (green), compared to the blank (black). All data was normalized to the pressure of each sample.

range, the production of gases did not depend on current density but only on the total charge passed, thus no threshold for degradation dependent upon current density was observed.

The oxidized samples at +5 mA for varied time produced hydrogen and trifluoromethane, Fig. 4 represents only eight hours of oxidation. If there was any production of butane/butene from the oxidation of the IL, it was at the analytical detection limit. The majority of butane/butene produced would be from the reduction half-cell. In contrast to the reductive degradations, there was no relationship observed between hydrogen production and the amount of oxidizing charge. Trifluoromethane was present at a much lower yield from oxidation than from reduction, but was still clearly related to the total charge passed.

Samples of $[\text{N}_{4,1,1,1}][\text{Tf}_2\text{N}]$ with 0.5 M lithium bis(trifluoromethylsulfonyl)imide ($\text{Li}[\text{Tf}_2\text{N}]$) diluted with equal volumes of acetonitrile were degraded to compare gaseous products with and without Li^+ present. The mass spectra from the degradation samples with Li^+ present are similar to those without Li^+ , as shown in Fig. 5. The same gas peaks are present in the samples from reductive degradation at m/z of 50.1 through 59.1 amu, 69.1 amu, and 101.4 amu. In further comparison of the systems with Li to those without, it was observed that the addition of lithium ion decreased the production of all of the observed products formed from reduction, except for trifluoromethane. The Li ion is reduced to the metal in this system,

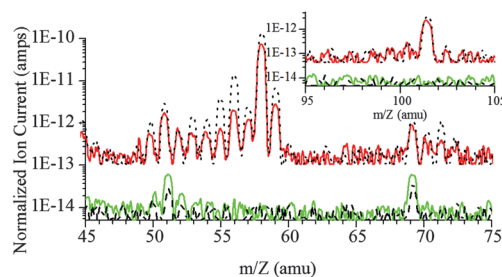


Fig. 5 Effect of lithium ions on the degradation of $[\text{N}_{4,1,1,1}][\text{Tf}_2\text{N}]$ for 8 hours at +5 mA (green, solid) and -5 mA (red solid) with 0.5 M Li; and without Li (black, dashed[+] and dotted [-]). The product spectra from reduction are offset by a factor of 10. Spectra are normalized to individual sample pressures.

hence decreasing the reduction efficiency of the $[\text{N}_{4,1,1,1}]^+$ into alkyl and amine products. The trifluoromethane product results from degradation through direct oxidation of the $[\text{Tf}_2\text{N}]^-$ or from indirect degradation of the $[\text{Tf}_2\text{N}]^-$ during reduction of the IL.

In the samples from oxidative degradation with Li^+ in solution (Fig. 5) there are common peaks at m/z of 51.1 and 69.1 amu, both of which have been attributed to trifluoromethane.

GC-MS analysis

The $[\text{N}_{4,1,1,1}][\text{Tf}_2\text{N}]$ was degraded with -5 mA for 8 hours, and the chromatogram of the gas sample is shown in Fig. 6 with significant peaks numbered. The first peak (peak 1) appears to be broad, and begins as a shoulder of the most intense peak in the chromatogram and through mass spectrum was confirmed to be trifluoromethane.

The fragmentation patterns for peaks 2, 3, and 5 are identical and match those for *cis*- and *trans*-2-butene and 2-methylpropene. With column separations being roughly based on the boiling point, peak 2 would be 2-methylpropene (b.p. = -6.9 °C), peak 3 *trans*-2-butene (b.p. = 0.8 °C), peak 5 is *cis*-2-butene (b.p. = 4 °C), and peak 6 is butane. Peak 4 appearing at 3 minutes was assigned to 2-methylprop-1-en-1-amine, as shown in Fig. 7. This assignment was made based on the molecular ion at $m/z = 71$, and the base peak at $m/z = 55$ corresponding to a loss of NH_2 .

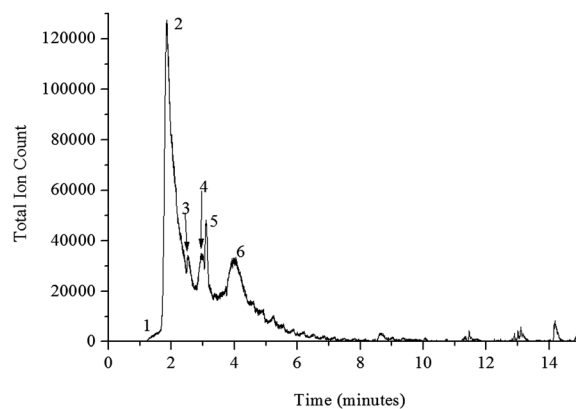


Fig. 6 Total ion count versus time for $[\text{N}_{4,1,1,1}][\text{Tf}_2\text{N}]$ degraded with -5 mA for 8 hours.

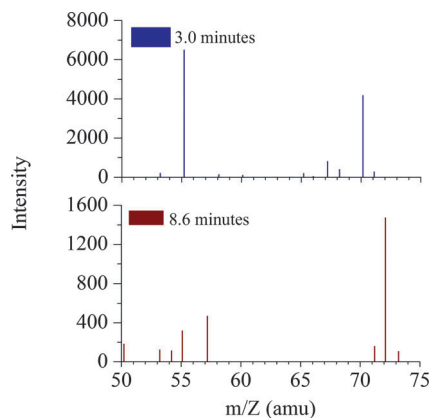


Fig. 7 Mass spectra for peak 4 at 3 minutes (top) identified as 2-methylprop-1-en-1-amine, and a peak at 8.6 minutes (bottom) identified as butan-1-amine. Background has been subtracted.

Another amine, eluting at 8.6 minutes, is shown and identified in Fig. 7 as butan-1-amine. This product is identified based on the molecular ion at $m/z = 73$, the loss of NH_2 leading to the peak at $m/z = 57$, and the typical butyl fragmentation pattern.

Eluting at 14.2 minutes was a product predicted to be *N*-ethyl-*N*-methylbutan-1-amine, as shown in Fig. 8. This assignment was made based on the molecular ion at $m/z = 114$, and the base peak at $m/z = 57$ corresponding to a butyl fragment. The fragment at $m/z = 72$ is again a butan-1-amine ($-\text{H}$), and the peak at $m/z = 85$ corresponds to a loss of an ethyl group from the *N*-ethyl-*N*-methylbutan-1-amine. This product is thought to result from a rearrangement reaction of the $[\text{N}_{4,1,1,1}]^+$ within the electrochemical cell yielding the charge neutral amine.

FTIR analysis

The absorbance spectrum of a gas sample from $[\text{N}_{4,1,1,1}][\text{TF}_2\text{N}]$ degraded with -5 mA for 8 hours was measured in a 10 cm path length cell, equilibrated to atmospheric pressure. The resulting spectrum, shown in Fig. 9, was analysed using a database from Infrared Analysis, Inc. and the Aldrich Library of FT-IR Spectra.²¹ Methane was identified by the peaks at 3113, 3017, 2927, and 1306 cm^{-1} and the associated rotational bands. The sensitivity of methane is greater in the FTIR measurements than the mass-spectrometry based analysis. Butane was assigned to the 2968, 2877, and 1464 cm^{-1} peaks. The peaks at 3334 (and rotational bands), 1671, 1625, 1122, 1046, 992, 966,

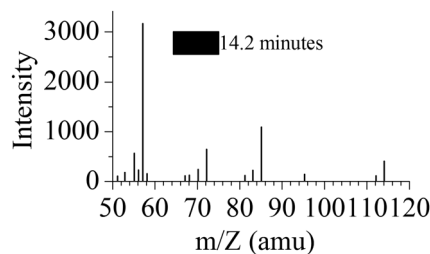


Fig. 8 Mass spectrum for a product eluting at 14.2 minutes, identified as *N*-ethyl-*N*-methylbutan-1-amine.

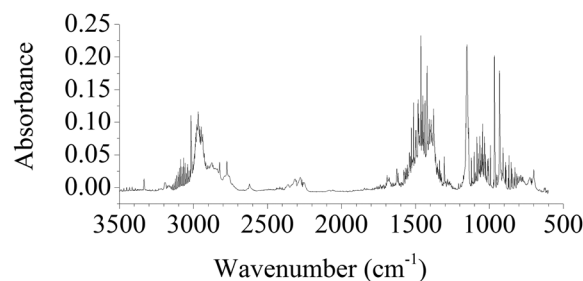


Fig. 9 FT-IR spectra of non-condensable gas degradation products formed from -5 mA over 8 hours in $[\text{N}_{4,1,1,1}][\text{TF}_2\text{N}]$ in a 10 cm path length cell. Identified products include: ammonia, methane, butane, trimethylamine, trifluoromethane, and acetonitrile used to dilute the ionic liquid and increase conductivity.

931, 908, and 868 cm^{-1} were assigned to ammonia. Acetonitrile (diluent) was observed at several peaks including 2988, 2622, 1554, 1514, 1421, 1377, 1337, 1059, and 716 cm^{-1} with the neighbouring broad peaks. Overlapping with one of the broad acetonitrile peaks near 716 cm^{-1} is a peak at 700 cm^{-1} , which along with peaks at 1152, 1208, and 3035 cm^{-1} are attributed to trifluoromethane. Trimethylamine is also assigned to the peaks at 2962, 2823, 2774, 1457, 1271, 1179 (as a shoulder of the 1152 cm^{-1} peak), and 1050 cm^{-1} . Some low and broad absorbance peaks remain at 1692, 1635, 1380, 895, and 789 cm^{-1} which at this point have not been identified.

Hydrogen production as a function of water content

The hydrogen observed under reducing conditions could result from radical reactions within the ionic liquids, or from the reduction of water. All ILs will maintain some hydrated water in them. In order to better understand the source of the hydrogen, the same IL system was 'doped' with water and held under similar reducing conditions. The dried IL had been measured for water content by Karl Fischer titration, and was found to contain 52.5 ± 2.1 ppm of water. Analysis in the literature has shown the water content of saturated $[\text{N}_{4,1,1,1}][\text{TF}_2\text{N}]$ to be 14 000 ppm.²² As seen in Fig. 10, there does seem to be a maximum rate of hydrogen production. Other researchers have observed a plateau effect at higher water concentrations for hydrogen production from water electrolysis in a different ILs, which they attributed to the solubility limit of water.²³

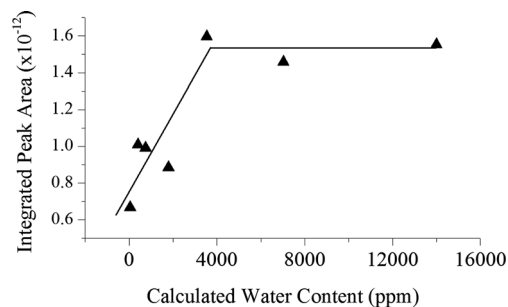


Fig. 10 Hydrogen production from dried $[\text{N}_{4,1,1,1}][\text{TF}_2\text{N}]$, water saturated $[\text{N}_{4,1,1,1}][\text{TF}_2\text{N}]$, and intermediate concentrations, with the integrated peak area of hydrogen ($m/z = 2.01$) plotted versus water content.

A different study in acidic IL attributed lower rates of hydrogen production to the slow Volmer reaction, being the simultaneous electron transfer to a proton and its adsorption to the electrode surface.²⁴ Because the samples studied for hydrogen production were below the saturation limit of water, the plateau effect is most likely due to rate limitations of the charge transfer reaction, but further study is needed for conclusive evidence. However, the important findings are that in practical applications, even the driest of ILs will still retain some water leading to additional hydrogen production, and that even an ionic liquid with no water would still lead to the reductive formation of hydrogen gas.

Conclusions

The electrochemical degradation of $[N_{4,1,1,1}][Tf_2N]$ in acetonitrile produces flammable gases, greenhouse gases, and noxious and toxic gases within short exposure times not too far out of standard Li/Li^+ potentials. With the exception of trifluoromethane, all gaseous by-products originate from the cation, $[N_{4,1,1,1}]^+$, summarized in Table 1. The source of all nitrogen-based compounds was the quaternary ammonium cation, as there was no observed evidence of sulphur-based compounds supporting further degradation of the anions.

The presence of dissolved water increases the production of hydrogen *via* electrolysis, but ILs will also produce hydrogen due to internal reduction. In reducing environments, the presence of lithium ion decreases the electrochemical degradation of the IL due to lithium metal deposition on the working electrode. In the cases of overpotentials or depletion of Li^+ , the rate of gaseous production from degradation of the IL will increase.

With proper system design and controls, ILs could remain viable for commercial use in Li/Li^+ systems. Where ILs would be used as an electrolyte in a Li/Li^+ system, the highly conductive nature of the ILs, with no measureable vapour pressure still provides them as a viable option for commercial use.

Table 1 Gaseous degradation products from dried $[N_{4,1,1,1}][Tf_2N]$. Masses in parentheses correspond to products only observed by FT-IR. Masses in brackets were only observed by GC-MS. All other products were observed using DI-MS in combination with data from GC-MS, FTIR, and literature information

Product mass on DI-MS (<i>m/z</i>)	Reductive degradation product	Secondary method of confirmation
2.01	Hydrogen	N/A
(16.0)	Methane	FTIR
(17.0)	Ammonia	FTIR
51.1	Trifluoromethane	GC-MS, FTIR
55.1	2-Butene, 2-methylpropene	GC-MS
56.1	2-Butene, 2-methylpropene	GC-MS
57.1	Butane	GC-MS, FTIR
58.1	Butane, trimethylamine	GC-MS, FTIR
59.1	Trimethylamine	FTIR
69.1	Trifluoromethane	GC-MS, FTIR
70.1	2-Methylprop-1-en-1-amine	GC-MS
71.2	2-Methylprop-1-en-1-amine	GC-MS
72.2	Butan-1-amine	GC-MS
[73.0]	Butan-1-amine	GC-MS
101.4	<i>N,N'</i> -Dimethylbutylamine	GC-MS
[114.0]	<i>N</i> -Ethyl- <i>N</i> -methylbutan-1-amine	GC-MS

Experimental

Electrochemical degradation

An H-cell was designed and made by the SRNL Glass Shop such that gas samples could be drawn into a pre-evacuated bottle from one side of the apparatus. The $[N_{4,1,1,1}][Tf_2N]$ purchased from IoLiTec was diluted with an equal volume of acetonitrile and decolorized with activated carbon equal to a tenth of the IL mass. The suspension was filtered, and the cleaned $[N_{4,1,1,1}][Tf_2N]$ was dried at 90 °C under argon flow, then the pressure was reduced until a constant volume was achieved.

Equal volume ratios of dry acetonitrile from Sigma-Aldrich with $[N_{4,1,1,1}][Tf_2N]$ were used to dilute the IL. A platinum foil working electrode of approximately 4 mm by 16 mm by 0.2 mm was lowered halfway into the IL, and a larger piece of platinum foil was used as the counter electrode. At least 8 hours were allowed for complete wetting of the Vycor frit before the experiment was started. A PAR273A potentiostat was used with CorrWare software.

At the end of the degradation run the pre-evacuated bottle was opened collecting the non-condensable gases from the headspace at sub-atmospheric pressures. Blank samples were also collected, where all conditions were the same except no current was passed through the system. For the lithium loaded systems, dry $Li[Tf_2N]$ salt from Sigma-Aldrich was used to prepare 0.5 M solutions of Li in $[N_{4,1,1,1}][Tf_2N]$.

Gas analysis (DI-MS)

An OmniStar GSD 320 O2C mass spectrometer with an yttriated iridium filament was used for gas analysis. The mass spectrometer was run using Quadera software in scan mode from 1 to 199 amu (*m/z*) at 200 ms amu⁻¹ and a resolution of 5. Background scans were taken with nitrogen purge gas flowing for three scans before analyzing each sample over three scans. The sample pressures above the mass spectrometer isolation valve were at least 2 psia, and did not vary during analysis by more than 0.01 psia. The sample signal was calculated as the difference between the average of the background scans taken just prior to the samples and the average of the sample scans. Spectra were analyzed by normalizing the sample signal to the gas pressure.

Gas analysis (GC-MS)

The headspace samples were analyzed by purge and trap Gas Chromatography-Mass Spectroscopy (GC-MS) by injecting the gases into the purge system during the purge cycle. Analytical separations were carried out on a Hewlett Packard 6890 gas chromatograph, equipped with a 20 m DB-624 column with 0.18 mm diameter and 1.0 μm film thickness. Gas samples were injected directly into a water purge system, so water soluble products such as ammonia, light amines, and methane would not be carried through onto the GC column. Species with *m/z* < 50 amu were also excluded from the collected data due to experimental background. Quantitation was performed using a Hewlett Packard 5973 mass selective detector. Initial chromatograms were obtained by injecting 1 mL gas samples without splitting the injection. The injection port was held at 200 °C and

the column flow was 0.5 mL min⁻¹. The oven temperature was held at 27 °C for eight min at injection then raised at 20 °C min⁻¹ up to 200 °C. The mass spectrometer electron multiplier was set for 1200 volts for the initial chromatographic measurements.

Gas analysis (FT-IR)

A 10 cm path length glass cell was purged with nitrogen gas, and sealed with rubber gaskets. The 10 cm cell was placed in the sampling chamber of a Nicolet 6700, and a background spectrum was collected using 1 cm⁻¹ resolution, triangular apodization, and 512 scans. An empty syringe was inserted to partially evacuate the glass cell, removed, and the sample syringe was inserted and sample was backfilled into the cell. A rubber gasket was briefly opened to equilibrate the sample pressure to atmospheric pressure. All data was collected at room temperature and atmospheric pressure. Automatic CO₂ and H₂O subtraction was performed by the OMNIC software on the instrument. During data analysis spectral subtraction was performed with the Essential FT-IR program as components were identified, if matched standard spectra were available.

Acknowledgements

Savannah River National Laboratory is operated by Savannah River Nuclear Solutions. This manuscript has been authored by Savannah River Nuclear Solutions, LLC under Contract No. DEAC09-08SR22470 with the U.S. Department of Energy. The United States Government retains and the publisher, by accepting this article for publication, acknowledges that the United States Government retains a non-exclusive, paid-up, irrevocable, worldwide license to publish or reproduce the published form of this work, or allow others to do so, for United States Government purposes.

References

- 1 Y. Ein-Eli, S. F. McDevitt and R. Laura, *J. Electrochem. Soc.*, 1998, **145**, L1.
- 2 W. H. Meyer, *Adv. Mater.*, 1998, **10**, 439.
- 3 E. B. Fox, A. E. Visser, N. J. Bridges and J. W. Amoroso, *Energy Fuels*, 2013, **27**, 3385.
- 4 S. Pohlman, B. Lobato, T. A. Centeno and A. Balducci, *Phys. Chem. Chem. Phys.*, 2013, **15**, 17827.
- 5 A. Brandt, C. Ramirez-Castro, M. Anouti and A. Balducci, *J. Mater. Chem. A*, 2013, **1**, 12669.
- 6 D. R. MacFarlane, N. Tachikawa, M. Forsyth, J. M. Pringle, P. C. Howlett, G. D. Elliott, J. H. Davis, M. Wantanabe, P. Simon and C. A. Angell, *Energy Environ. Sci.*, 2014, **7**, 232.
- 7 E. T. Fox, E. Paillard, O. Borodin and W. A. Henderson, *J. Phys. Chem. C*, 2013, **117**, 78.
- 8 S. Menne, R.-S. Kühnel and A. Balducci, *Electrochim. Acta*, 2013, **90**, 641.
- 9 M. Buzzeo, C. Hardacre and R. Compton, *ChemPhysChem*, 2006, **7**, 176.
- 10 E. I. Rogers, B. Sljukic, C. Hardacre and R. Compton, *J. Chem. Eng. Data*, 2009, **54**, 2049.
- 11 P. C. Howlett, E. I. Izgorodina, M. Forsyth and D. R. MacFarlane, *Z. Phys. Chem.*, 2006, **220**, 1483.
- 12 M. C. Kroon, W. Buijs, C. J. Peters and G.-J. Witkamp, *Green Chem.*, 2006, **8**, 241.
- 13 Y.-H. Tian, G. S. Goff, W. H. Runde and E. R. Batista, *J. Phys. Chem. B*, 2012, **116**, 11943.
- 14 P. Kurzweil and M. Chwistek, *J. Power Sources*, 2008, **176**, 555.
- 15 J. A. Vega, J. Zhou and P. A. Kohl, *J. Electrochem. Soc.*, 2009, **156**, A253.
- 16 R. Wibowo, S. E. W. Jones and R. G. Compton, *J. Chem. Eng. Data*, 2010, **55**, 1374.
- 17 N. J. Bridges, A. E. Visser, M. J. Williamson, J. I. Mickalonis and T. M. Adams, *Radiochim. Acta*, 2010, **98**, 243.
- 18 J. Sun, M. Forsyth and D. R. MacFarlane, *J. Phys. Chem. B*, 1998, **102**, 8858.
- 19 D. Behar, P. Neta and C. Schultheisz, *J. Phys. Chem. A*, 2002, **106**, 3139.
- 20 I. A. Shkrob, S. D. Chemerisov and J. F. Wishart, *J. Phys. Chem. B*, 2007, **111**, 11786.
- 21 C. J. Pouchert, *The Aldrich Library of FT-IR Spectra*, Aldrich Chemical Company, Milwaukee, 1st edn, 1989, vol. 3.
- 22 J. Jacquemin, P. Husson, A. A. H. Padua and V. Maier, *Green Chem.*, 2006, **8**, 172.
- 23 R. F. de Souza, J. C. Padilha, R. S. Gonçalves and J. Tault-Berthelot, *Electrochem. Commun.*, 2006, **8**, 211.
- 24 Y. Meng, L. Aldous, S. R. Belding and R. G. Compton, *Phys. Chem. Chem. Phys.*, 2012, **14**, 5222.